



## Abstract

Linking landslide size and frequency is important at both human and geological time-scales for quantifying both landslide hazards and the effectiveness of landslides in the removal of sediment from evolving landscapes. Landslide inventories are usually compiled following a particular triggering event such as an earthquake or storm, and their statistical behavior is typically characterized by an inflected power-law relationship. The occurrence of landslides is expected to be influenced by the material properties of rock and/or regolith in which failure occurs. Here we explore the statistical behavior and the controls of a secular landslide inventory (SLI) (i.e. events occurring over an indefinite time period) consisting of mapped landslide deposits and their underlying lithology (bedrock or superficial) across the United Kingdom. The magnitude-frequency distribution of this secular inventory exhibits an inflected power law relationship, well approximated by an inverse Gamma or double Pareto model. The scaling exponent for the power-law relationship is  $\alpha = -1.76$ . The small-event rollover occurs at a significantly higher magnitude than observed in single-event landslide records, which we interpret as evidence of “landscape annealing” at these relatively short length-scales, noting the corollary that a secular dataset will tend to underestimate the frequency of small landslides. This is supported by a subset of data where a complete landslide inventory was recently mapped. Large landslides also appear to be under-represented relative to model predictions, which we interpret as a non-linear or transient landscape response as the UK emerged from the last glacial maximum and through relatively volatile conditions toward a generally more stable late Holocene climate.

## 1 Introduction

This paper describes the generation and analysis of a secular landslide inventory (SLI) derived from the UK National Landslide Database (Foster et al., 2012). We tackle the basic questions: do secular landslides reflect the same or different statistical properties

# ESurfD

1, 113–139, 2013

## Scaling of a secular landslide inventory

M. D. Hurst et al.

Title Page

Abstract

Introduction

Conclusions

References

Tables

Figures

◀

▶

◀

▶

Back

Close

Full Screen / Esc

Printer-friendly Version

Interactive Discussion



## Scaling of a secular landslide inventory

M. D. Hurst et al.

Title Page

Abstract

Introduction

Conclusions

References

Tables

Figures

◀

▶

◀

▶

Back

Close

Full Screen / Esc

Printer-friendly Version

Interactive Discussion



as generally better known single-event driven landslides, and what role is played by the underlying lithology and type of landslide? The drivers for the current analysis include the need to quantify landslide hazards and to better understand erosional processes in long-term landscape evolution.

5 Landslides pose a significant hazard to human life and infrastructure. In the US, Japan, Italy and India landslides have been estimated to result in economic losses for each in excess of (1990 US dollars) \$1.0 billion per annum (Schuster, 1996). Between 2004 and 2010 there were 2600 fatal landslides globally, with 32 000 associated fatalities (Petley, 2012). Whilst loss of life due to landsliding in the UK is relatively rare, 10 landslides pose a risk to infrastructure and are relevant in land use planning (Gibson et al., 2012). Landslides also have the potential to disrupt transport links (Winter et al., 2010), and land use change has been acknowledged to influence the occurrence of landslides throughout the world (Glade, 2003). To the extent that landslide behavior is in part dictated by levels and frequency characteristics of precipitation, there is concern 15 that the patterns and severity of landsliding may be affected by future climate change (Crozier, 2010; Keiler et al., 2010; Korup et al., 2012).

Landslides are important geomorphic processes which generate and transport significant volumes of rock, regolith and soil (e.g. Larsen et al., 2010; Korup et al., 2010). Landslides occur in a variety of styles, dictated by a web of interrelated factors, including material properties (e.g. soil type and thickness, bedrock type, the orientation 20 and spacing of discontinuities), landscape morphology (e.g. slope, topographic convergence, aspect) and climate (e.g. freeze-thaw and shrink-swell cyclicality, pore-water pressures). Whilst large landslides are often perceived to be most hazardous, small landslides occur most frequently; therefore quantifying the size-frequency distribution for landslide events is important to the assessment of landside hazard and to land use 25 planning (Malamud et al., 2004). Landslides may also be a significant component of the sediment budget in a landscape and hence understanding their size-frequency characteristics is important to studies of long-term landscape evolution (Stark and Guzzetti, 2009).

## Scaling of a secular landslide inventory

M. D. Hurst et al.

Title Page

Abstract

Introduction

Conclusions

References

Tables

Figures

◀

▶

◀

▶

Back

Close

Full Screen / Esc

Printer-friendly Version

Interactive Discussion



Several studies have established that the frequency of landslides (i.e. the number of slides occurring over a given length of time or within a given area) for medium to large events follows a heavy-tailed, negative power-law relationship with landslide size (e.g. Hovius et al., 1997; Pelletier et al., 1997; Stark and Hovius, 2001; Guzzetti et al., 2002; Turcotte et al., 2002). Estimates of the exponent  $\alpha$  for power-law scaling of large events vary from  $\alpha \approx 1.0$  (Hovius et al., 1997) up to  $\alpha \approx 2.5$  (Stark and Hovius, 2001; Turcotte et al., 2002), and Malamud et al. (2004) suggested  $\alpha \approx 2.4$  might be universally applicable based on consensus between three contrasting event-driven datasets. There is also evidence that scaling may vary with underlying geology (e.g. Guzzetti et al., 2008) and the type of failure event (Dussauge et al., 2003).

A power-law model typically only holds for larger events, with landslide size-frequency distributions from around the world consistently exhibiting a rollover to a positive relationship for small landslides (e.g. Brardinoni and Church, 2004; Malamud et al., 2004; Guzzetti et al., 2008). The rollover has been interpreted in some cases as the existence of a minimum critical size, i.e. a potential landslide must exceed a critical size in order for the shear stress acting on a plane of weakness to overcome resisting forces (Pelletier et al., 1997; Guzzetti et al., 2002). Alternatively (or perhaps additionally), the rollover has been attributed to the under-sampling of small landslides when compiling the inventory. Under-sampling might occur due to evidence of small landslides being rapidly healed through recolonization by vegetation (Brardinoni and Church, 2004), difficulties in identification of smaller landslides, or resolution issues with remotely sensed datasets (Stark and Hovius, 2001; Malamud et al., 2004).

Two statistical distributions have been proposed to model the rollover in size-frequency distributions. Stark and Hovius (2001) found landslide inventories from New Zealand and Taiwan could be fit by a double Pareto distribution. Malamud et al. (2004) favor fitting an inverse gamma function which can also account for the rollover. An inverse gamma function provided a good approximation of the size frequency distribution of datasets from Italy, Guatemala and USA, with different trigger conditions (snow melt, storm and earthquake triggers, respectively) (Malamud et al., 2004). The three

inventories were considered to be complete (i.e. the rollover is real and not a result of under-sampling of small landslides) thereby leading Malamud et al. (2004) to suggest the model as a general fit for any complete event-driven landslide inventory.

The universality of such a general model for landslide distributions has not been verified, nor has its applicability to historic, multi-trigger-event inventories yet been thoroughly demonstrated. However, if a general model is appropriate to all events in a secular inventory then the probability distribution should also satisfy the sum of all events. By comparison to the proposed general distribution, the total number of landslides associated with a particular trigger can be established even for an incomplete landslide inventory (Malamud et al., 2004). Recent studies of historic inventories (e.g. Guzzetti et al., 2008; Rossi et al., 2010; Trigila et al., 2010) show similar power-law scaling with  $\alpha \approx 2.1$ – $2.4$  but with the location of the roll-over offset towards larger landslides. Guzzetti et al. (2008) interpret that the offset as due to difficulty in documenting smaller landslides from aerial photos and their tendency to amalgamate, but which might also relate to the loss of smaller landslides from the record due to landscape annealing by reworking of deposits and recolonization by vegetation. Such an analysis has not until now been performed on a secular inventory spanning a large spatial and temporal range.

The concept of a general model for a landslide size-frequency relationship may seem at odds with the range of factors expected to influence landslide occurrence, such as climate, vegetation, material properties of bedrock/regolith and the type/style of failure. Clarke and Burbank (2010) compared the size-frequency distribution of two landslide inventories in Fiordland and the Southern Alps in New Zealand, which are dominated by igneous and high-grade metamorphic lithologies, and low-grade metamorphic lithologies, respectively. Whilst power-law scaling exponents were similar between the two sites ( $\alpha \approx 1.07$  and  $1.16$ , respectively), the sizes of the largest landslides were roughly an order of magnitude larger, and the position of the rollover in frequency was also shifted toward larger landslides in the Southern Alps compared to Fiordland. Dussauge et al. (2003) analysed inventories of rock falls in the Sierra Nevada, California

## Scaling of a secular landslide inventory

M. D. Hurst et al.

Title Page

Abstract

Introduction

Conclusions

References

Tables

Figures

◀

▶

◀

▶

Back

Close

Full Screen / Esc

Printer-friendly Version

Interactive Discussion



## Scaling of a secular landslide inventory

M. D. Hurst et al.

Title Page

Abstract

Introduction

Conclusions

References

Tables

Figures

◀

▶

◀

▶

Back

Close

Full Screen / Esc

Printer-friendly Version

Interactive Discussion



and French Alps and found that the scaling exponent was significantly lower than those reported for landslide inventories compiled for assorted landslide types ( $\alpha \approx 0.5$ ). This would suggest that a general model for the distribution of landslides may not take into account lithologic variability and differences in the type of mass movement processes (which are likely linked themselves). With these two notable exceptions there seems to be a lack of studies relating the size-frequency distribution of landslides to the type of material failing and the style of mass movement.

In a recent review, Guzzetti et al. (2012) recognized that detailed inventories of landslides are lacking, advocating them as a vital tool in assessing susceptibility and risk at a variety of time and length-scales. Inventories may focus at a variety of temporal and spatial scales, from a single drainage basin (Guzzetti et al., 2008) to national scale (Trigila et al., 2010); from single event-triggered landslide clusters (Parker et al., 2011) to multi-temporal historical records (Galli et al., 2008) with unconstrained landslide ages. In this study, we attempt to quantify and explain the statistical properties of a national-scale secular landslide inventory, test the geomorphic completeness (i.e. degree of landscape annealing) of such an inventory and estimate the number of landslides that might be missing from the geomorphic record. We link the frequency distribution of landslide sizes to the lithology or deposits in which they occur to assess whether particular lithologies may have been more prone to landsliding. Finally we select landslides in which the type of failure was known in order to assess whether scaling relationships are a function of landslide type. We achieve this by generating a national-scale secular landslide inventory (SLI) from the National Landslide Database (NLD) in the United Kingdom, mapped landslide deposits, and underlying geology.

## 2 Data and methods

### 2.1 Landslide data

The National Landslide Database (NLD) is an extensive inventory of ancient and recent landslides in the UK (Fig. 1) (Foster et al., 2012). The database is managed by the British Geological Survey (BGS), having inherited and expanded a database initially compiled from secondary sources by Geomorphological Services Limited in the late 1980s, on behalf of the UK Government's Department of the Environment (Jones and Lee, 1994). The NLD comprises a series of points ( $N = 16808$ ; November 2012) recording the location of known landslides, the precise timing of which is often unknown. Many of these points have been through a quality assurance (QA) procedure ( $N = 13108$ ; November 2012) verifying their location by reference to previous studies, maps or field surveys.

The NLD includes a detailed record of many attributes of a particular landslide event including landslide type, slide material, presence of vegetation, hillslope gradient and estimated age (see Foster et al., 2012 for further details), but the availability of this data depends on when and by whom the individual landslide was recorded. During QA the points are related to mapped landslide deposits recorded by geological mapping at 1 : 10000 and 1 : 50000 scales over the last century by the BGS (British Geological Survey, 2009, 2010). The continuing collection, updating and verification of landslide information by the BGS is vital to planning and development within the UK (Foster et al., 2012), and is a fundamental component in the nationwide assessment of landslide susceptibility (Walsby, 2008).

### 2.2 Sampling methods

The magnitude-frequency relationship for landslides in the UK was quantified based on linking quality assured landslides in the NLD (Fig. 1) to their associated mapped landslide deposits, where available, using GIS software. We emphasize that in this

## Scaling of a secular landslide inventory

M. D. Hurst et al.

Title Page

Abstract

Introduction

Conclusions

References

Tables

Figures

◀

▶

◀

▶

Back

Close

Full Screen / Esc

Printer-friendly Version

Interactive Discussion



**Scaling of a secular landslide inventory**

M. D. Hurst et al.

Title Page

Abstract

Introduction

Conclusions

References

Tables

Figures

◀

▶

◀

▶

Back

Close

Full Screen / Esc

Printer-friendly Version

Interactive Discussion



contribution we are analyzing the *deposit area* rather than the total failure plus run-out area as is more commonly reported (Malamud et al., 2004), because landslide deposit areas only have been recorded as part of BGS's geological mapping.

During the quality assurance procedure, if a landslide reported in the NLD can be allied to a mapped landslide deposit, the coordinates of the point record in the NLD are moved to the location of highest elevation at the edge of the mapped landslide polygon. In some cases where the head scarp of the landslide is visible in aerial photographs or topographic data, the point coordinates in the NLD will alternatively be moved to the highest point on the observed scarp. In order to link points in the NLD to mapped landslide polygons we used ArcGIS software to measure the shortest distance between records in the NLD and their nearest deposit area polygon. Where this distance was less than 50 m we considered that the point and polygon are related and hence attributes of the mapped landslide deposit polygons could be linked to the NLD (e.g. Fig. 2; box 2) to generate the sample used in the current analysis.

There were a number of caveats to this linking procedure requiring consideration. Firstly, mapped deposits may consist of the amalgamation of several proximal landslide run-outs, or be the result of landslide reactivation and therefore have multiple associated events in the NLD (e.g. Fig. 2; box 1). In order to isolate individual event deposits, we filtered out records where multiple points from the NLD were associated with a single landslide deposit polygon ( $N = 1944$ ). Similarly, we filtered occurrences of a landslide deposit polygon that had no associated nearby ( $< 50$  m) records in the NLD ( $N = 1177$ ). We also filtered records in the NLD with no associated mapped landslide deposit (Fig. 2; red points,  $N = 6026$ ). Finally, we also filtered coastal landslides (via a 500 m buffer from the UK coastline) in order to restrict our analysis to strictly terrestrial landslides ( $N = 386$ ). The resulting sampled dataset consists of 8452 single landslide event-deposit area pairs. We subsequently refer to this filtered landslide dataset to as the Secular Landslide Inventory (SLI).

To quantify landslide size, we used ArcGIS to measure the aerial extent of each mapped landslide deposit polygon retained in the SLI. We used the centroid points of

## Scaling of a secular landslide inventory

M. D. Hurst et al.

Title Page

Abstract

Introduction

Conclusions

References

Tables

Figures

◀

▶

◀

▶

Back

Close

Full Screen / Esc

Printer-friendly Version

Interactive Discussion



mapped deposit polygons to sample the underlying lithology and the presence/absence of superficial material from digital geological maps (British Geological Survey, 2009, 2010), following the BGS's standardised rock classification scheme (RCS) (Styles et al., 2006). The geology of the United Kingdom is quite diverse, with over 180 separate RCS codes identified during sampling. In order to look for lithologic control on landslides, we split these into seven broad lithologic groups: superficial deposits, mudstones, interbedded sedimentary units, coarse clastic sedimentary units (sandstones and coarser), carbonates, metamorphics and igneous (Table 1).

### 2.3 Statistical analysis

The frequency density ( $F_D$ ) of a landslide inventory is given by the number of landslides  $N$  over the range of areas  $dA$ . Probability density ( $P_D$ ) can be defined for a landslide dataset as  $F_D$  normalised to the total number of landslides in the inventory  $N$  according to:

$$P_D = \frac{1}{N} F_D = \frac{1}{N} \frac{N}{dA} \quad (1)$$

in which  $P$  is the probability of a landslide with area  $A$  [ $L^2$ ] (Malamud et al., 2004). We calculated  $F_D$  and  $P_D$  for the NLD dataset by sorting the data into logarithmically-spaced bins in  $A$ . As previously noted, the scaling of probability with landslide size for medium-large landslides can be described by a power-law:

$$P_D = bA^\alpha \quad (2)$$

Where  $b$  is a coefficient and  $\alpha$  is a dimensionless scaling exponent. Stark and Hovius (2001) proposed using a double Pareto model to describe the size distribution of observed landslides, which accounts for under-sampling of smaller landslides. In the model the probability density  $P(A)$  is a function of two exponents,  $\alpha_p$  and  $\beta$ , which describe the rate of decay for large and small landslides, respectively, either side of a

peak landslide area  $A_{\text{peak}}$ :

$$P(A) = \frac{\alpha_p}{A_{\text{peak}}} \times \frac{\left[ \left( \frac{A_{\text{max}}}{A_{\text{peak}}} \right)^{-\beta} \right]^{\frac{\alpha_p}{\beta}}}{\left[ \left( \frac{A}{A_{\text{peak}}} \right)^{-\beta} \right]^{1 + \frac{\alpha_p}{\beta}}} \times \frac{A^{-\beta-1}}{A_{\text{peak}}} \quad (3)$$

where  $A$  is landslide area [ $L^2$ ],  $A_{\text{max}}$  is the largest landslide in the dataset [ $L^2$ ],  $A_{\text{peak}}$  is the area at which the rollover occurs [ $L^2$ ],  $\alpha_p$  is the exponent controlling negative power-law scaling for  $A_{\text{peak}} < A < A_{\text{max}}$ , and  $\beta$  is the exponent controlling positive power-law scaling when  $0 < A < A_{\text{peak}}$  (Stark and Hovius, 2001). Note that the negative power law scaling  $\alpha$  is equivalent to  $\alpha_p + 1$ . Similarly, Malamud et al. (2004) modelled the probability density of a landslide inventory with a three-parameter inverse Gamma function, which acts as an inverse power-law for medium-large landslides:

$$P(A) = \frac{1}{r\Gamma(\alpha_g)} \left( \frac{r}{A-s} \right)^{\alpha_g+1} \exp \frac{r}{A-s} \quad (4)$$

where  $\alpha_g$  is the exponent setting the inverse power-law scaling for large landslides (again note that  $\alpha$  is equivalent to  $\alpha_g + 1$ ),  $r$  [ $L^2$ ] is a parameter controlling the location of the peak in the probability distribution and  $s$  [ $L^2$ ] controls the rate of decay for small landslide areas.

### 3 Results

The size-frequency distribution of the SLI is shown in Fig. 3. The probability distribution of landslides increases with landslide area, peaking at  $1.0\text{--}7.0 \times 10^{-3} \text{ km}^2$ , before diminishing in a power-law fashion (Fig. 3a). Previously documented event-driven landslide inventories show similar humped probability distributions (Brardinoni and Church,

## Scaling of a secular landslide inventory

M. D. Hurst et al.

Title Page

Abstract

Introduction

Conclusions

References

Tables

Figures

◀

▶

◀

▶

Back

Close

Full Screen / Esc

Printer-friendly Version

Interactive Discussion



## Scaling of a secular landslide inventory

M. D. Hurst et al.

Title Page

Abstract

Introduction

Conclusions

References

Tables

Figures

◀

▶

◀

▶

Back

Close

Full Screen / Esc

Printer-friendly Version

Interactive Discussion



2004; Guzzetti et al., 2008; Malamud et al., 2004; Pelletier et al., 1997; Stark and Hovius, 2001). A double Pareto distribution (Stark and Hovius, 2001) and a truncated inverse Gamma function (Malamud et al., 2004), have also been plotted in Fig. 3a using maximum likelihood estimates to find the best fit parameters. These functions coincide well with the observed probability distribution for UK landslides at areas  $< 10^0 \text{ km}^2$ , although there is discrepancy between the data and model distributions for the largest mapped deposits. The median landslide size is  $15.3 \times 10^{-3} \text{ km}^2$  and the most frequent landslides are of the order  $10^{-3}$  to  $10^{-2} \text{ km}^2$ . Figure 3a also shows the general distribution model postulated by Malamud et al. (2004) attributed to complete landslide inventories associated with a trigger event (earthquake or storm). The SLI is offset by roughly an order of magnitude with respect to the peak probability for the size of landslides, indicating fewer small landslides ( $< 10^{-2} \text{ km}^2$ ) in the SLI compared to event-driven landslides. In contrast to the frequency distribution (Fig. 3b), the general model of Malamud et al. (2004) is able to produce a reasonable fit for the largest landslides in the dataset ( $> 10^0 \text{ km}^2$ ) with  $N = 10^6$ . The implications of this alternative fit will be discussed in Sect. 4.

We subdivided the SLI into broad lithologic groups (Fig. 4a) sampled from BGS 1 : 50 000 scale geological maps (British Geological Survey, 2010). The majority of landslides occur in superficial material, or clastic sedimentary rocks, particularly fine grained clays and muds and fines interbedded with coarser units. Based on the abundance of landslides (Table 1) and the distribution in Fig. 4a we refer to these as less-resistant lithologies. Landslides in carbonates, metamorphic and igneous units make up a relatively small part of the dataset (see Table 1) and we refer to these as more resistant lithologies. Small landslides ( $< 10^{-2} \text{ km}^2$ ) are most abundant in superficial deposits, but medium-large landslides are more common in clastic sedimentary bedrock.

For more resistant lithologic groups there are similar numbers of large landslides ( $\approx 10^0 \text{ km}^2$ ) as there are in clastic sedimentary rocks, but smaller landslides are relatively infrequent. We quantified these trends by fitting a power-law relationship of the form of Eq. (2) to the binned data by lithology for landslides in the range

$10^{-2} < A < 10^0 \text{ km}^2$ . Table 1 shows the fitted parameters  $\alpha$  and  $b$  determined by maximum likelihood estimation and regression statistics for log-transformed data. Gradient ( $b$ ) is highest for landslides in superficial deposits reflecting the abundance of small landslides and relative scarcity of larger events. Our data indicate that landslides in more resistant lithologies, particularly those of igneous origin, have much lower fitted gradients and therefore a proportionately greater number of large landslide events.

In order to assess the relative susceptibility of these lithologic groups to landsliding, we compare values of the intercept  $a$  for a best-fit, fixed, normalizing exponent ( $\alpha = -1.76$ ) taken from the dataset as a whole (Table 1). We find that mudstones are most vulnerable to medium-large landslides, followed closely by interbedded units, coarse clastic units and then superficial deposits. Of the more resistant lithologies, carbonates and metamorphics are similarly prone to landsliding whilst igneous lithologies are least susceptible.

Finally, a subset of the SLI was plotted where information about the type of mass movement process was available ( $N = 854$ ). Figure 4b shows the probability distribution for the four most common types of landslide; rotational slides ( $N = 373$ ), planar slides ( $N = 303$ ), flows ( $N = 131$ ), and falls/topples ( $N = 47$ ). Despite a much smaller sample size, these categories still display roll-over-power-law scaling for the landslide size-frequency relationship. The median event size decreases from rotational slides ( $A = 0.058 \text{ km}^2$ ) to planar slides ( $A = 0.033 \text{ km}^2$ ) and down to flow events ( $A = 0.021 \text{ km}^2$ ). This is perhaps not unexpected as rotational landslides tend to be large deep-seated events involving significant amounts of bedrock, whilst flows tend to be hydraulically driven and mobilize material at the near-surface. Whilst the sample size is small, the gradient of the best fit line for falls/topples is low (exponent  $\alpha = -0.57$ ) similar to the findings of Dussauge et al. (2003).

## Scaling of a secular landslide inventory

M. D. Hurst et al.

Title Page

Abstract

Introduction

Conclusions

References

Tables

Figures

◀

▶

◀

▶

Back

Close

Full Screen / Esc

Printer-friendly Version

Interactive Discussion



## 4 Discussion

Whilst we do not present a complete dataset of all landslide occurrences in the UK, several features emerge from the results that speak to difference and similarities between event-driven and secular landslide inventories, and to the important part that geology plays, each of which have implications for landslide hazard management.

### 4.1 Landscape annealing and the small-landslide rollover

Comparison of the SLI magnitude-frequency relationship (Fig. 3) to the expected, general distribution for event-triggered landslides (Malamud et al., 2004, Fig. 3a, dashed line) reveals an order of magnitude offset between the peak areas. We interpret this to indicate the relative incompleteness of the SLI due to underrepresentation of small landslides. The causes behind this likely include difficulties in recognizing small events in the field due to recolonization by vegetation or subsequent redistribution of the deposit. We note that the NLD is not a complete landslide inventory and is constantly growing with the addition of newly observed historic landslides and new landslides (Foster et al., 2012). Mapping of landslide deposits as part of the geological mapping program at the BGS is a continuing process and it is not expected that a complete coverage of landslide deposits in the UK has yet been achieved. This is demonstrated by a number of events in the NLD that did not link to an associated mapped deposit (Fig. 2) and hence did not make it into the SLI.

To test the extent to which small landslides are underrepresented, we analyzed separately a subset of the landslides data recently mapped in the North Yorkshire Moors, which are considered to be a complete historic inventory (Fig. 5). The area at which peak probability is observed is only slightly offset between the North Yorkshire dataset (2660 m<sup>2</sup>) and the SLI (3100 m<sup>2</sup>), compared to the order of magnitude offset observed in relation to the general distribution proposed by Malamud et al. (2004). We suggest this slight difference may relate to the completeness of these datasets, with the likelihood that there are some smaller events in the NLD that were filtered out when

## Scaling of a secular landslide inventory

M. D. Hurst et al.

Title Page

Abstract

Introduction

Conclusions

References

Tables

Figures

◀

▶

◀

▶

Back

Close

Full Screen / Esc

Printer-friendly Version

Interactive Discussion



compiling the SLI (Fig. 3). We stress, however, that there remains a large offset between the SLI and the general event based model proposed by Malamud et al. (2004), suggesting that this offset is real and likely the result of landscape annealing due to the loss of evidence of small events from the landscape. This is consistent with the reasonable likelihood that landslides were more active during the uppermost Pleistocene to lower Holocene (e.g. Ballantyne, 2002) such that many smaller and early landslides have had significant time to heal (see further discussion below on landslide timing).

## 4.2 Role of lithology

Landslides in superficial deposits and soft lithologies dominate the SLI, whilst harder lithologic groups exhibit distinct magnitude frequency scaling characterized by lower values of  $\alpha$  setting lower scaling gradient in log-log space (Fig. 4a; Table 1). This result has important implications for landslide size and associated hazard. Whilst there is significantly lower probability of small landslides in more resistant lithologies, the difference is minimal for larger landslides ( $\approx 10^0 \text{ km}^2$ ). Perhaps unsurprisingly the largest proportion of landslides and in particular smaller landslides ( $< 10^{-3} \text{ km}^2$ ) occurs in poorly consolidated superficial deposits and hence characterization of superficial materials will be important to site-based investigation of landslide susceptibility. Magnitude-frequency scaling of landslides classified by the type of mass movement have power-law scaling exponents ( $\alpha = -0.95$  to  $-1.5$ ) lower than the dataset as a whole ( $\alpha = -1.76$ ). Lower exponents suggest that the subset of data may be biased towards larger events, and indeed it seems likely (and reasonable) that detailed field studies to determine the style of failure are preferentially carried out for larger failure events. There are few observations of landslide type below areas of  $10^{-3} \text{ km}^2$  (Fig. 4b) yet there are a large number of landslides in the NLD of this magnitude (Fig. 3b).

## Scaling of a secular landslide inventory

M. D. Hurst et al.

Title Page

Abstract

Introduction

Conclusions

References

Tables

Figures

◀

▶

◀

▶

Back

Close

Full Screen / Esc

Printer-friendly Version

Interactive Discussion



### 4.3 The large-landslide deficit

A national landslide inventory for Italy comprising 377 k landslides (Trigila et al., 2010) exhibits power-law scaling above  $10^{-2} \text{ km}^2$  similar to the SLI (Fig. 3a). Interestingly both datasets show deviation from fitted scaling relationships for the largest landslides ( $> 10^0 \text{ km}^2$  for the UK;  $> 10^1 \text{ km}^2$  in Italy) suggesting that either we are under-sampling with respect to the largest landslides or large events are less frequent than power-law scaling would predict. The difference in cutoff areas between the two datasets may be the result of only reporting the areas of mapped deposits in the UK whilst in Italy area refers to the combined source and sink outline. We predicted the number of large landslides expected by inverting Eq. (1) for  $N$  for the fitted inverse gamma function (using the same binning scheme as for the landslide data). Comparison to the SLI suggests a deficit of  $\approx 150$  landslides of size  $> 0.5 \text{ km}^2$ , or  $> 100\%$  of the observed number of landslides within this binned category ( $N = 139$ ). It seems unlikely that this many relatively large landslides have been missed, and we suggest that the deficit is real. The deficit may, in fact, be larger, as inspection shows that some of the largest mapped deposit areas consist of amalgamated deposits of numerous smaller events.

A possible explanation for the apparent deficit of relatively large landslides (Fig. 3a) is related to a temporal transience of landslide activity across the UK. It is likely that the bulk of landslides range in age from the last glacial maximum (21 ka) to the present-day. During this time, climate related forcing will have varied as the British Ice Sheet receded (Clark et al., 2012), and mass movement processes are likely to have been initially more active as soils and regolith both warmed and lost structural support from ice-cover and permafrost. We speculate, therefore, that many landslides and certainly most of the larger landslides would occur early in this last glacial maximum (LGM) to present time-span, and that the drivers for those landslides are gradually reduced over time as the emerging landscape passes through a period of readjustment to new and more stable conditions (Ballantyne, 2002). Instability likely continued through the volatile climate immediately prior to the Holocene, and returned again during the latter

## Scaling of a secular landslide inventory

M. D. Hurst et al.

Title Page

Abstract

Introduction

Conclusions

References

Tables

Figures

◀

▶

◀

▶

Back

Close

Full Screen / Esc

Printer-friendly Version

Interactive Discussion



## Scaling of a secular landslide inventory

M. D. Hurst et al.

Title Page

Abstract

Introduction

Conclusions

References

Tables

Figures

◀

▶

◀

▶

Back

Close

Full Screen / Esc

Printer-friendly Version

Interactive Discussion



part of the Holocene (Neolithic times, in particular) as extensive anthropogenic forest clearance and land-use changes occurred. These latter processes, all else being equal, would lead to an increase in the rate of landslide activity, consistent with rapid Neolithic valley sedimentation observed in many parts of the UK (Brown, 2009). We suggest, therefore, that the population of landslides in the SLI is dominated by the relatively rapid denudation of early post-LGM and early anthropogenic times, with the result that relatively large landslides show a deficit with respect to a model-fit that is derived principally from the relatively greater number of smaller to moderate sized landslides.

An alternative perspective is provided by the area-frequency analysis (Fig. 3b), which would suggest that large-landslide deficit is only apparent, and that it is smaller and moderate-sized landslides that are in deficit. To reach this conclusion would require the assumption that the general model proposed by Malamud et al. (2004) was appropriate to represent the probability density for all landslides in the UK since the LGM. Moreover it would suggest that the landscape annealing processes by which small events are lost from the geomorphic record not only act to offset the position of the “hump” in historic landslide inventories, but also reduce the exponent  $\alpha$  through time. Data for historic inventories presented by Malamud et al. (2004) (after Guzzetti et al., 2003; Ohmori and Sugai, 1995) suggest that this is not the case because  $\alpha$  appears to be conserved in those historic inventories. Thus it remains unclear whether the model of Malamud et al. (2004) is appropriate to a secular landslide inventory spanning several thousand years and a highly variable external forcing, during which time there is reason to suspect variation in the frequency (and possibly size) of landslides.

### 4.4 Implications for landslide hazards

The combined results here have implications for the assessment of landslide hazards and ultimately for landslide risk management. At face value, for example, the model-fit presented here yields a low probability of small landslides relative to other landslide databases. This size category includes anything from 10 to 30 m in equivalent radius, which can be hazardous to a wide variety of infrastructure. It is more likely, however,

**Scaling of a secular landslide inventory**

M. D. Hurst et al.

Title Page

Abstract

Introduction

Conclusions

References

Tables

Figures

◀

▶

◀

▶

Back

Close

Full Screen / Esc

Printer-friendly Version

Interactive Discussion



that the secular record of landslides presented here significantly under-represents landslides of this size, as we argue above. In other words, the national-scale, small-landslide hazard is greater than predicted by the model fit to the SLI (Fig. 3a, Table 1). Our results also tell us that the probability of landslides of any particular size is largely independent of type (i.e. scaling between size and frequency still follows a power law with rollover), but that type and magnitude are linked, with deep-seated rotational landslides tending to be larger than planar slides and flows. The role of lithology emerges as control by two broad classes of bedrock (resistant: carbonates, metamorphic and igneous rocks vs. less resistant: superficial, mudstones, interbedded, and coarse clastics) each characterized by a distinct power-law distribution and each (with the exception of igneous rocks) showing a rollover at relatively small landslides. We also suggest that the discrepancy between model and observations for relatively large landslides is a function of a transient landslide response as the UK emerged from glacial conditions and into an initially volatile then stable climate. In other words, the national-scale large-landslide hazard is lower than predicted by the model fit to the SLI (Fig. 3a and Table 1). It is important to emphasize that the SLI is a sample only of the whole national landslide database (itself an incomplete record of all past landslides in the UK), and that it does not include coastal landslides. Implications drawn from the present analysis of the SLI should not be applied in a local or regional analysis nor to any specific landslide in the UK.

## 5 Conclusions

A statistical analysis of a national (UK) secular landslide inventory reveals an inverse Gamma or double Pareto distribution with a well-defined rollover at a landslide area between  $10^{-3}$  to  $10^{-2}$  m<sup>2</sup>. The power-law component for medium-large landslides has a scaling exponent  $\alpha = -1.76$ . The general form of the distribution is similar to that found for many single-event driven landslides, although there are two important specific differences. First: the magnitude of the small-landslide rollover occurs at a significantly

## Scaling of a secular landslide inventory

M. D. Hurst et al.

Title Page

Abstract

Introduction

Conclusions

References

Tables

Figures

◀

▶

◀

▶

Back

Close

Full Screen / Esc

Printer-friendly Version

Interactive Discussion



larger size than in single-event samples. We interpret as a reflection of a landscape annealing process (e.g. recolonization by vegetation, reactivated or modified in later landslides), with the corollary that the model fit underestimates the frequency of relatively small landslides. Second: we observe a deficit, relative to the model fit, in the largest landslides. We interpret this as a temporal transience or non-linear response of the UK landscape as it emerged from the LGM and passed through a relatively volatile climate state and, during the Neolithic, accelerated landscape change due to human activity. Thus, we suggest that most of the landslides, certainly the larger ones, are likely to have formed early in the post-LGM time-span as the soil-regolith-bedrock column lost support of both ice and/or permafrost. The corollary is that the model fit overestimates the frequency of relatively large landslides. Landslides grouped by multiple lithologies behave as two distinct groups, providing a potential for a simple approach to landslide-behavioural parameterization in models of landscape evolution, with shallow landslides developed in superficial materials show a tendency toward a relatively high  $\alpha \approx -2.1$ .

*Acknowledgements.* We thank Claire Dashwood, Catherine Pennington and Helen Reeves for contributions which greatly improved the sampling techniques and interpretations presented here. Thanks also to Ken Lawrie for assistance with the NLD. We are also grateful for discussion with Bruce Malamud. This paper is published with the permission of the Executive Director of the British Geological Survey.

## References

- Ballantyne, C.: Paraglacial geomorphology, *Quaternary Sci. Rev.*, 21, 1935–2017, 2002. 126, 127
- Brardinoni, F. and Church, M.: Representing the landslide magnitude-frequency relation: Capilano River basin, British Columbia, *Earth Surf. Proc. Land.*, 29, 115–124, 2004. 116, 122
- British Geological Survey: Digital Geological Map of Great Britain 1:10 000 scale (DiGMapGB-10) data. Version 2.18., Keyworth, Nottingham: British Geological Survey., Release date 15-01-2009, 2009. 119, 121

## Scaling of a secular landslide inventory

M. D. Hurst et al.

Title Page

Abstract

Introduction

Conclusions

References

Tables

Figures

◀

▶

◀

▶

Back

Close

Full Screen / Esc

Printer-friendly Version

Interactive Discussion



- British Geological Survey: Digital Geological Map of Great Britain 1:50 000 scale (DiGMapGB-50) data. Version 6.20., Keyworth, Nottingham: British Geological Survey., Release date 14-10-2010, 2010. 119, 121, 123
- 5 Brown, A.: Colluvial and alluvial response to land use change in Midland England: An integrated geoaerchaeological approach, *Geomorphology*, 108, 92–106, 2009. 128
- Clark, C. D., Hughes, A. L. C., Greenwood, S. L., Jordan, C., and Sejrup, H. P.: Pattern and timing of retreat of the last British-Irish Ice Sheet, *Quaternary Sci. Rev.*, 44, 112–146, 2012. 127
- 10 Clarke, B. A. and Burbank, D. W.: Bedrock fracturing, threshold hillslopes, and limits to the magnitude of bedrock landslides, *Earth Planet. Sc. Lett.*, 297, 577–586, doi:10.1016/j.epsl.2010.07.011, 2010. 117
- Crozier, M.: Deciphering the effect of climate change on landslide activity: A review, *Geomorphology*, 124, 260–267, 2010. 115
- 15 Dussauge, C., Grasso, J., and Helmstetter, A.: Statistical analysis of rockfall volume distributions: Implications for rockfall dynamics, *J. Geophys. Res.-Sol. Ea.*, 108, 2286, doi:10.1029/2001JB000650, 2003. 116, 117, 124
- Foster, C., Pennington, C. V. L., Culshaw, M. G., and Lawrie, K.: The National Landslide Database of Great Britain : development, evolution and applications, *Environ. Earth Sci.*, 66, 941–953, doi:10.1007/s12665-011-1304-5, 2012. 114, 119, 125
- 20 Galli, M., Ardizzone, F., Cardinali, M., Guzzetti, F., and Reichenbach, P.: Comparing landslide inventory maps, *Geomorphology*, 94, 268–289, 2008. 118
- Gibson, A., Culshaw, M., Dashwood, C., and Pennington, C.: Landslide management in the UK – the problem of managing hazards in a “low-risk” environment, *Landslides*, 1–12, doi:10.1007/s10346-012-0346-4, 2012. 115
- 25 Glade, T.: Landslide occurrence as a response to land use change: a review of evidence from New Zealand, *Catena*, 51, 297–314, 2003. 115
- Guzzetti, F., Malamud, B. D., Turcotte, D. L., and Reichenbach, P.: Power-law correlations of landslide areas in central Italy, *Earth Planet. Sc. Lett.*, 195, 169–183, 2002. 116
- 30 Guzzetti, F., Reichenbach, P., Cardinali, M., Ardizzone, F., and Galli, M.: The impact of landslides in the Umbria region, central Italy, *Nat. Hazards Earth Syst. Sci.*, 3, 469–486, doi:10.5194/nhess-3-469-2003, 2003. 128

## Scaling of a secular landslide inventory

M. D. Hurst et al.

Title Page

Abstract

Introduction

Conclusions

References

Tables

Figures

◀

▶

◀

▶

Back

Close

Full Screen / Esc

Printer-friendly Version

Interactive Discussion



- Guzzetti, F., Ardizzone, F., Cardinali, M., Galli, M., Reichenbach, P., and Rossi, M.: Distribution of landslides in the Upper Tiber River basin, central Italy, *Geomorphology*, 96, 105–122, 2008. 116, 117, 118, 123
- Guzzetti, F., Mondini, A., Cardinali, M., Fiorucci, F., Santangelo, M., and Chang, K.: Landslide inventory maps: New tools for an old problem, *Earth-Sci. Rev.*, 112, 42–66, 2012. 118
- Hovius, N., Stark, C. P., and Allen, P. A.: Sediment flux from a mountain belt derived by landslide mapping, *Geology*, 25, 231–234, 1997. 116
- Jones, D. and Lee, E.: *Landsliding in Great Britain*, Department of the Environment, London, 1994. 119
- Keiler, M., Knight, J., and Harrison, S.: Climate change and geomorphological hazards in the eastern European Alps, *Philos. T. R. Soc. A*, 368, 2461–2479, 2010. 115
- Korup, O., Densmore, A., and Schlunegger, F.: The role of landslides in mountain range evolution, *Geomorphology*, 120, 77–90, 2010. 115
- Korup, O., Görüm, T., and Hayakawa, Y.: Without power? Landslide inventories in the face of climate change, *Earth Surf. Processes*, 37, 92–99, 2012. 115
- Larsen, I., Montgomery, D., and Korup, O.: Landslide erosion controlled by hillslope material, *Nat. Geosci.*, 3, 247–251, 2010. 115
- Malamud, B. D., Turcotte, D. L., Guzzetti, F., and Reichenbach, P.: Landslide inventories and their statistical properties, *Earth Surf. Processes*, 29, 687–711, 2004. 115, 116, 117, 120, 121, 122, 123, 125, 126, 128, 137, 139
- Ohmori, H. and Sugai, T.: Toward geomorphometric models for estimating landslide dynamics and forecasting landslide occurrence in Japanese mountains, *Zeitschrift Fur Geomorphologie Supplementband*, 101, 149–164, 1995. 128
- Parker, R., Densmore, A., Rosser, N., De Michele, M., Li, Y., Huang, R., Whadcoat, S., and Petley, D.: Mass wasting triggered by the 2008 Wenchuan earthquake is greater than orogenic growth, *Nature Geosci.*, 4, 449–452, 2011. 118
- Pelletier, J. D., Malamud, B. D., Blodgett, T., and Turcotte, D. L.: Scale-invariance of soil moisture variability and its implications for the frequency-size distribution of landslides, *Eng. Geol.*, 48, 255–268, 1997. 116, 123
- Petley, D.: Global patterns of loss of life from landslides, *Geology*, 40, 927–930, 2012. 115
- Rossi, M., Witt, A., Guzzetti, F., Malamud, B. D., and Peruccacci, S.: Analysis of historical landslide time series in the Emilia-Romagna region, northern Italy, *Earth Surf. Proc. Land.*, 35, 1123–1137, 2010. 117

## Scaling of a secular landslide inventory

M. D. Hurst et al.

Title Page

Abstract

Introduction

Conclusions

References

Tables

Figures

◀

▶

◀

▶

Back

Close

Full Screen / Esc

Printer-friendly Version

Interactive Discussion



- Schuster, R. L.: Socioeconomic Significance of Landslides, chap. 2, 12–35, National Academies Press, Transportation Research Board Special Report, 1996. 115
- Stark, C. P. and Guzzetti, F.: Landslide rupture and the probability distribution of mobilized debris volumes, *J. Geophys. Res.*, 114, F00A02, doi:10.1029/2008JF001008, 2009. 115
- 5 Stark, C. P. and Hovius, N.: The characterization of landslide size distributions, *Geophys. Res. Lett.*, 28, 1091–1094, 2001. 116, 121, 122, 123
- Styles, M., Gillespie, M., Bauer, W., and Lott, G.: Current status and future development of the BGS Rock Classification Scheme, Tech. rep., British Geological Survey, this item has been internally reviewed but not externally peer-reviewed, 2006. 121
- 10 Trigila, A., Iadanza, C., and Spizzichino, D.: Quality assessment of the Italian Landslide Inventory using GIS processing, *Landslides*, 7, 455–470, 2010. 117, 118, 127
- Turcotte, D. L., Malamud, B. D., Guzzetti, F., and Reichenbach, P.: Self-organization, the cascade model, and natural hazards, *P. Natl. Acad. Sci. USA*, 99, 2530–2537, 2002. 116
- Walsby, J.: *GeoSure; a bridge between geology and decision-makers*, Geological Society, London, Special Publications, 305, 81–87, 2008. 119
- 15 Winter, M., Dent, J., Macgregor, F., Dempsey, P., Motion, A., and Shackman, L.: Debris flow, rainfall and climate change in Scotland, *Q. J. Eng. Geol. Hydrogeol.*, 43, 429–446, 2010. 115

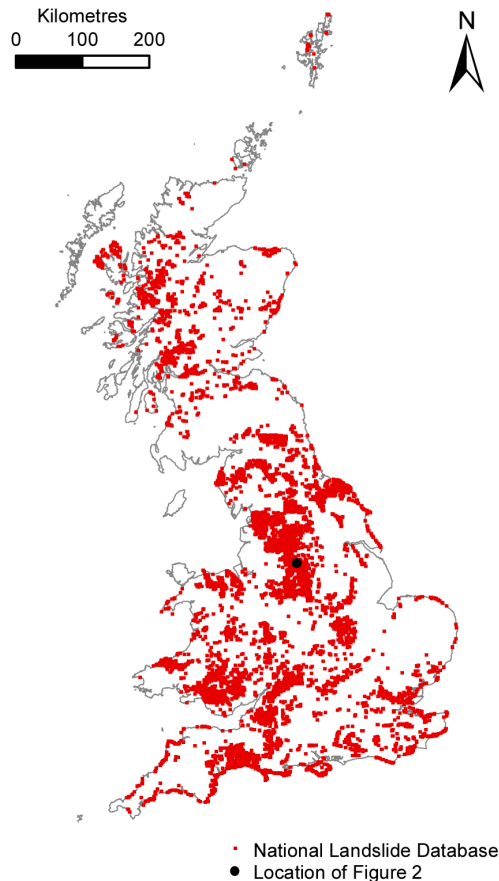
## Scaling of a secular landslide inventory

M. D. Hurst et al.

**Table 1.** Best fit parameters to power law function of the form  $P(A) = bA^\alpha$  for medium-large landslides in each lithologic group. Since  $b$  is dependent on the regression slope in log-log space, we also report best fit values for  $b$  for a normalising value of  $\alpha = -1.76$  taken from the dataset as a whole.  $R^2$  values are reported to log-transformed data fitted by maximum likelihood estimation.

Lithology	No. Landslides	$\alpha$	$b$	$R^2$	$b(\alpha = -1.95)$	$R^2$
Superficial	2497	-2.09	$50.2 \times 10^2$	0.96	$1.00 \times 10^2$	0.93
Mudstone	2339	-1.79	$2.42 \times 10^2$	0.97	$1.66 \times 10^2$	0.97
Interbedded	1986	-1.78	$1.72 \times 10^2$	0.97	$1.36 \times 10^2$	0.97
Clastic	1188	-1.67	$0.42 \times 10^2$	0.97	$1.13 \times 10^2$	0.96
Carbonate	268	-1.41	0.47	0.97	$0.27 \times 10^2$	0.92
Metamorphic	111	-1.19	0.04	0.93	$0.28 \times 10^2$	0.72
Igneous	64	-1.33	0.13	0.95	$0.16 \times 10^2$	0.86
(All)	(8453)	(-1.76)	$(5.60 \times 10^2)$	(0.98)	$(5.60 \times 10^2)$	(0.98)

[Title Page](#)
[Abstract](#)
[Introduction](#)
[Conclusions](#)
[References](#)
[Tables](#)
[Figures](#)
[I◀](#)
[▶I](#)
[◀](#)
[▶](#)
[Back](#)
[Close](#)
[Full Screen / Esc](#)
[Printer-friendly Version](#)
[Interactive Discussion](#)

**Fig. 1.** UK Map showing the distribution of landslide points in the National Landslide Database (NLD) which have undergone quality assurance control at the British Geological Survey. Open circle shows the location of Fig. 2.

**Scaling of a secular landslide inventory**

M. D. Hurst et al.

Title Page

Abstract Introduction

Conclusions References

Tables Figures

◀ ▶

◀ ▶

Back Close

Full Screen / Esc

Printer-friendly Version

Interactive Discussion



## Scaling of a secular landslide inventory

M. D. Hurst et al.

Title Page

Abstract

Introduction

Conclusions

References

Tables

Figures

◀

▶

◀

▶

Back

Close

Full Screen / Esc

Printer-friendly Version

Interactive Discussion

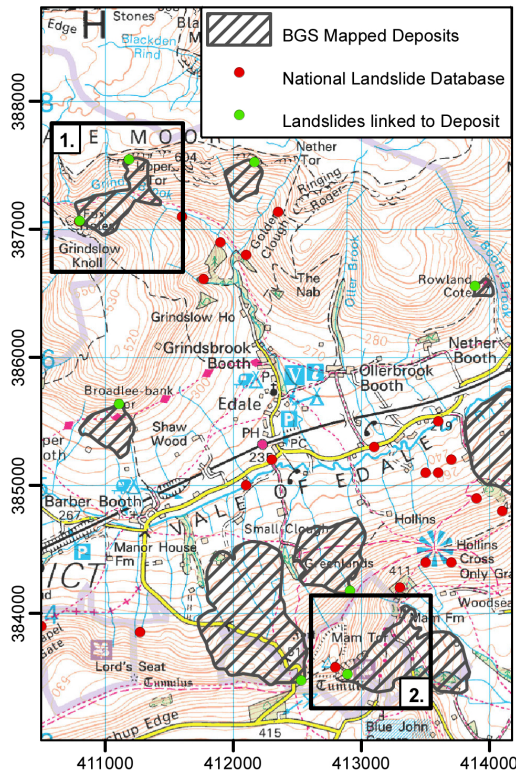


**Fig. 2.** Example map from the Vale of Edale in Derbyshire, showing the locations of points in the NLD (red), and mapped landslide deposits (hatched). Here, there were significantly more events in the database than there were polygons of mapped deposits, probably due to the scale at which mapping took place (1 : 50 000). Landslide events (red) with no associated, mapped deposit were removed from subsequent analysis. Box 1 highlights a scenario where a single mapped deposit polygon is a composite of two separate landslide events; hence these data are not included in later analysis. Box 2 shows an occasion where a landslide event (red) placed on the back scarp during Quality Assurance, has been associated with a nearby polygon and linked (green). The spatial reference system is British National Grid; the units are meters. OS topography © Crown Copyright. All rights reserved. 100017897/2010.

## Scaling of a secular landslide inventory

M. D. Hurst et al.

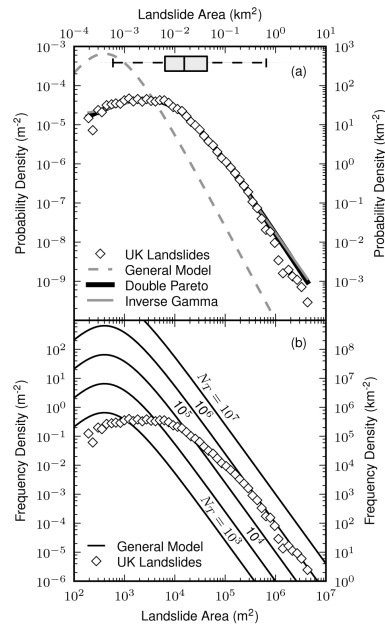


**Fig. 3.** (a) Probability distribution of landslide deposit area for landslides in the UK organized into logarithmically spaced bins (open diamonds). Solid black and grey lines show maximum likelihood estimates of a double Pareto function ( $\alpha_p = 0.95$ ;  $\beta = 1.68$ ;  $A_{\text{peak}} = 7730 \text{ m}^2$ ) and inverse Gamma function ( $\alpha_g = 0.85$ ;  $r = 9.75 \times 10^{-3} \text{ km}^2$ ;  $s = -2.16 \times 10^{-3} \text{ km}^2$ ), respectively. The dashed grey line is a proposed general distribution for landslides put forward by Malamud et al. (2004). Box plot shows the distribution statistics of area data with a median value of  $0.0153 \text{ km}^2$ . (b) Frequency density distribution for landslides in the UK. Solid lines represent the general distribution proposed by Malamud et al. (2004) for varying total number of landslides  $N_L$ .

## Scaling of a secular landslide inventory

M. D. Hurst et al.

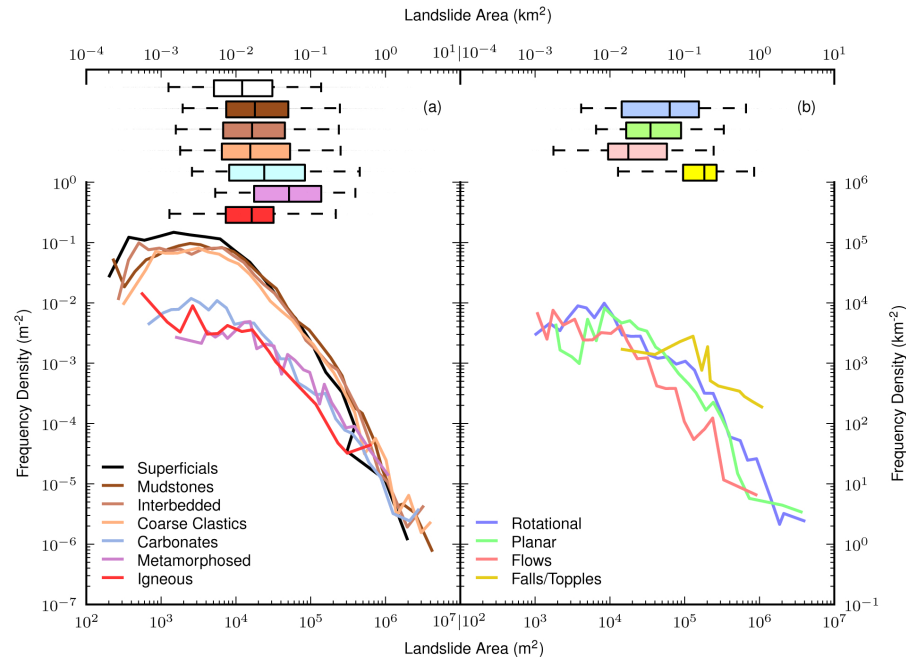


**Fig. 4.** (a) Frequency distributions classified into broad lithologic groups for logarithmically spaced bins. With the exception of the Igneous group, all lithologic groups exhibit power-law-roll-over scaling similar to the dataset as a whole as shown in (a). To quantify the relative susceptibility to landsliding of each of these groups we fitted a power law with a fixed gradient in logarithmic space ( $\alpha = -1.76$ ) and the best fit value of the coefficient  $b$  was determined (see Table 1). Box plots show the median and lower/upper quartile statistics of area data for each lithologic group (whiskers are 5th and 95th percentiles). (b) Frequency distributions classified by type of mass movement process; rotational slides, planar slides, flows and falls/topples. Box plots show the median and lower/upper quartile statistics of area data for each lithologic group (whiskers are 5th and 95th percentiles).

## Scaling of a secular landslide inventory

M. D. Hurst et al.

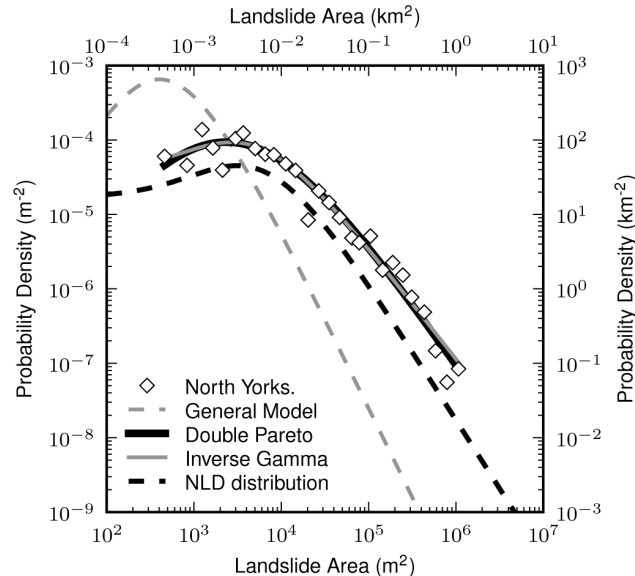


**Fig. 5. (a)** Probability distribution of landslide deposit area for landslides in North Yorkshire organized into logarithmically spaced bins (open diamonds). Solid black and grey lines show maximum likelihood estimates of a double Pareto function ( $\alpha_p = 0.69$ ;  $\beta = 2.61$ ;  $A_{\text{peak}} = 2533 \text{ m}^2$ ) and inverse Gamma function ( $\alpha_g = 0.51$ ;  $r = 6.47 \times 10^{-3} \text{ km}^2$ ;  $s = -1.64 \times 10^{-3} \text{ km}^2$ ) respectively, dashed grey and black lines show the general distribution proposed by Malamud et al. (2004) and the UK distribution from Fig. 3a, respectively. Note the similarity in shape between the North Yorkshire dataset and the NLD fit (the vertical offset in probability density, is due to a difference in the range of landslide sizes considered and does not indicate relative probability).

Title Page

Abstract

Introduction

Conclusions

References

Tables

Figures

◀

▶

◀

▶

Back

Close

Full Screen / Esc

Printer-friendly Version

Interactive Discussion

